minerals

MDPI

Article

Study on the Flotation Behavior of CMS-Na for Talc with Different Particle Sizes: Based on the Hydrophobicity Difference of Fracture Surfaces

Runqing Liu, Wenye Man, Wenchao Dong *, Yacong Wu and Zechao Huangfu

School of Minerals Processing and Bioengineering, Central South University, Changsha 410083, China; liurunqing@126.com (R.L.); 18797556131@163.com (W.M.); barcawu@126.com (Y.W.); huangfuzechao@163.com (Z.H.)

* Correspondence: dongwenchao2018@163.com

Abstract: Talc, as a phyllosilicate mineral, is often associated with sulfides such as copper, molybdenum, and nickel, which severely impact the flotation of target minerals. Micro-flotation experiments combined with SEM, contact angle, FTIR, TOC, and AFM analyses were performed to explore the influence and mechanism of sodium carboxymethyl starch (CMS-Na) on the flotation behavior of talc with varying particle sizes in a butyl xanthate system. The flotation results indicate that when CMS-Na is used as a depressant, the recovery of coarse talc particles (−74 + 45 μm) is only about 1%, while fine talc particles (−23 μm) maintain a recovery rate of over 70%. FTIR analysis revealed that the interaction between CMS-Na and talc involves both chemical and physical adsorption mechanisms, with the most pronounced effect observed on fine-grained talc surfaces. TOC, AFM, and contact angle measurements further revealed that the proportion of exposed edge surfaces increases as the talc particle size decreases. These edge surfaces exhibited a higher affinity for CMS-Na, resulting in significant reagent adsorption. Consequently, at an equivalent reagent dosage, the adsorption of CMS-Na on the basal planes was reduced, leading to the retention of high surface hydrophobicity. This phenomenon is considered an important factor contributing to the poor depressive effect on fine-grained talc.

Keywords: talc; different particle sizes; CMS-Na; inhibition mechanism

check for updates

Academic Editor: Przemyslaw B. Kowalczuk

Received: 24 March 2025
Revised: 5 April 2025
Accepted: 9 April 2025
Published: 11 April 2025

Citation: Liu, R.; Man, W.; Dong, W.; Wu, Y.; Huangfu, Z. Study on the Flotation Behavior of CMS-Na for Talc with Different Particle Sizes: Based on the Hydrophobicity Difference of Fracture Surfaces. *Minerals* **2025**, *15*, 402. https://doi.org/10.3390/min15040402

Copyright: © 2025 by the authors. Licensee MDPI, Basel, Switzerland. This article is an open access article distributed under the terms and conditions of the Creative Commons Attribution (CC BY) license (https://creativecommons.org/licenses/by/4.0/).

1. Introduction

Talc is a prevalent silicate mineral, often occurring in close association with pyrite and other silicate minerals. Talc has a chemical formula of $Mg_3(Si_4O_{10})(OH)_2$ and belongs to the TOT-type (2:1) layered silicate minerals. Its structure is characterized by an octahedral magnesium hydroxide (MgO) layer intercalated between two tetrahedral silica (SiO_4) layers, forming a characteristic T-O-T stacking sequence [1,2], as illustrated in Figure 1. The layers are bound by weak van der Waals interactions, making talc highly susceptible to interlayer cleavage during crushing and grinding, which leads to significant slime formation. Upon dissociation, talc demonstrates two distinct surface types: basal surfaces and edge surfaces. The basal surface is composed of inert siloxane (Si-O) groups, exhibiting nonpolar and hydrophobic characteristics. In contrast, the edge surface contains SiOH and MgOH functional groups, which are pH-sensitive and contribute to its hydrophilic nature [3–5]. Due to the predominant presence of basal surfaces, talc inherently exhibits high natural floatability [6,7], which allows it to inadvertently report to sulfide mineral flotation concentrates, thereby reducing the concentrate grade and increasing subsequent

metallurgical processing costs [8,9]. Therefore, selective depression of talc is essential to enhance its separation from valuable minerals, ultimately improving the quality of sulfide mineral concentrates [10,11].

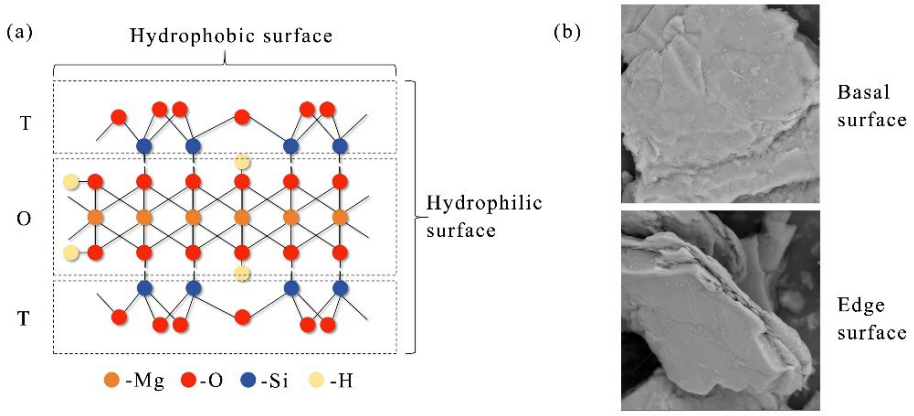


Figure 1. Schematic representation of talc's structure: (**a**) internal and (**b**) external.

Currently, talc depressants can be broadly categorized into inorganic and organic depressants [12–19]. Inorganic depressants primarily consist of sodium silicate (Na_2SiO_3) [20] and zinc sulfate ($ZnSO_4$) [13]. However, certain inorganic depressants, such as sodium silicate, exhibit poor selectivity for talc, potentially leading to the simultaneous depression of valuable minerals. Additionally, a relatively high dosage is often required in industrial applications to achieve effective talc depression, which limits their practical efficiency. In contrast, organic depressants have several advantages, including higher selectivity, minimal interference with target minerals, abundant availability, environmental friendliness, and cost-effectiveness. As a result, they have attracted increasing research interest in recent years, with numerous studies focusing on this category of depressants [21–28]. Among them, polysaccharide-based inhibitors are dominant, including carboxymethyl cellulose (CMC), chitosan, and lignosulfonates, which have shown promising results in selectively depressing talc flotation due to their ability to form stable complexes with talc surfaces. Huangfu Z. et al. [29] reported that sodium carboxymethyl starch (CMS-Na) exhibits a strong affinity for interaction with talc, facilitating its separation from molybdenite. Song S. et al. [30] found that adjusting the pH to 8.5 improved separation by increasing CMC adsorption on talc, reducing its floatability and enhancing chalcopyrite-talc separation. Pan G. et al. [31] found that under weakly alkaline conditions, the talc surface carries a negative charge, and CMC can further augment the negative charge on the talc surface, thereby enhancing the electrostatic repulsion between talc particles. This promotes talc dispersion in the slurry, leading to a reduction in its natural hydrophobicity and resulting in talc inhibition.

Although extensive research has been conducted on organic inhibitors for talc, studies on the differences in inhibitory effects across different particle sizes of talc are relatively limited. Given talc's tendency to over-grind and form fine particles in flotation, the particle size significantly influences the adsorption and inhibition behavior of reagents. Therefore, considering talc often coexists with copper-nickel sulfide ores, this study introduces butyl xanthate (BX), a commonly used collector for copper-nickel sulfide ores, and sodium carboxymethyl starch (CMS-Na) as an inhibitor, aiming to investigate the flotation performance of talc at varying particle sizes and its interaction with reagents in the presence of BX. The aim is to provide technical and theoretical references for further research on the efficient inhibition of talc from sulfide ores.

2. Materials and Methods

2.1. Minerals and Reagents

The talc sample used in the experiments was sourced from a talc deposit in Guilin, Guangxi. The raw talc ore was subjected to hand sorting, crushing, and ball milling with porcelain balls, followed by dry screening to obtain products of the particle sizes −74 + 45 μm, −45 + 23 μm, and −23 μm, which were used as experimental materials and stored in sealed containers. Figure 2 and Table 1 present the X-ray diffraction (XRD) pattern and chemical analysis data of the talc ore sample, respectively. As indicated by the results, the purity of the talc ore sample used in the experiment exceeded 90%, confirming it as a suitable monomineral for flotation experiments.

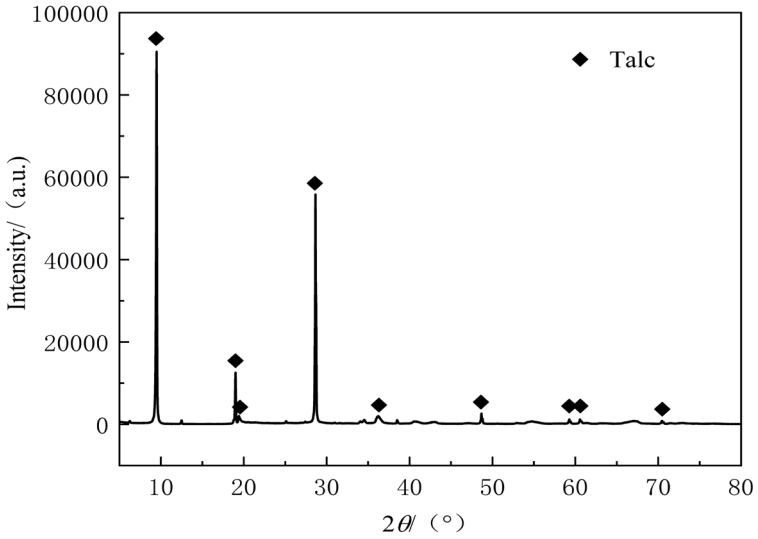


Figure 2. XRD pattern of talc.

The collector employed in the experiments was industrial-grade butyl xanthate (BX), while the frother used was methyl isobutyl carbinol (MIBC), and pH regulation was achieved with analytical-grade hydrochloric acid and sodium hydroxide. Sodium carboxymethyl starch (CMS-Na) served as the inhibitor, and deionized water was utilized throughout the experiments. The structure of sodium carboxymethyl starch is presented in Figure 3.

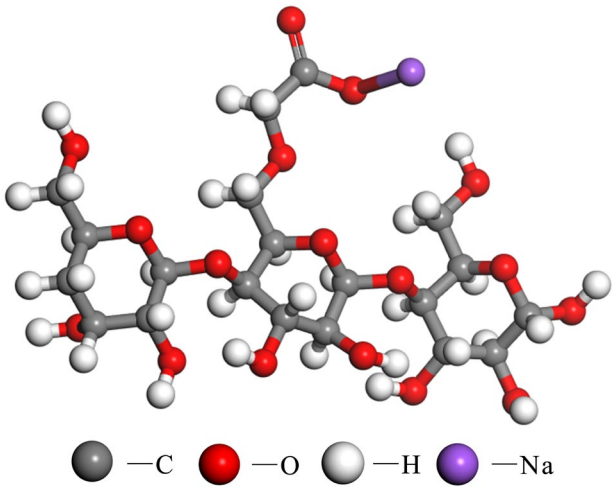


Figure 3. A schematic representation of the molecular structure of CMS-Na.

Table 1. Chemical analysis of talc.

Sample	Content (%)				
	MgO	**SiO_2**	**Fe**	**CaO**	**Other**
Talc	31.06	61.51	0.68	0.13	6.62

2.2. Flotation Experiments

The flotation experiment procedure is illustrated in Figure 4, which shows the experimental set-up and process flow. The flotation equipment type was XFG, with a rotational speed of 1900 rpm and a flotation cell volume of 40 mL, ensuring consistent agitation and froth formation. In each experiment, 2 g of talc needed to be placed into the flotation cell, followed by the addition of 40 mL of deionized water and stirring for 1 min. The pH of the pulp was then adjusted using hydrochloric acid or sodium hydroxide. Subsequently, the inhibitor and collector were added in sequence, with the inhibitor stirred for 2 min and the collector for 3 min. After adding the frother into the pulp for 1 min, the froth product then needed to be collected for 3 min. Then, both the froth product and the remaining pulp in the flotation cell were filtered, dried, and weighed to calculate the flotation recovery. Each experimental condition was replicated three times to ensure consistency, and the average value was used to minimize experimental error.

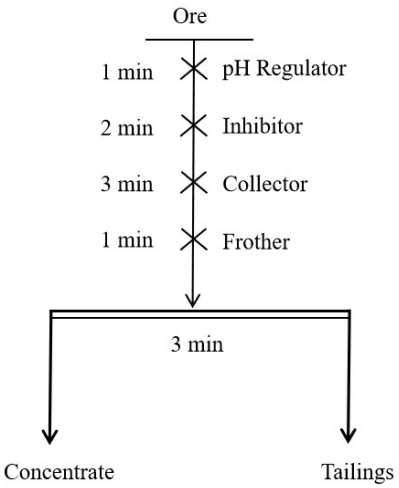


Figure 4. Flotation experimental flow.

2.3. FTIR Spectral Measurements

For the FTIR measurements, 2 g of talc was weighed and added to 40 mL of deionized water. We adjusted the pH to 9.5 and then added the corresponding reagents and stirred the mixture to allow a reaction. After the reaction, we filtered the mixture and rinsed the solid residue three times with deionized water. Subsequently, we dried the sample in a vacuum oven at 50 °C for 24 h. The dried sample was stored under vacuum conditions for subsequent analysis.

The FTIR measurements of the sample were performed using an IRAffinity infrared spectrometer. For the FTIR analysis, a small quantity of the sample was mixed with KBr at a 1:100 weight ratio, ground to achieve a particle size of less than 2 μm, and subsequently compressed into a pellet using a hydraulic press prior to analysis.

2.4. Total Organic Carbon (TOC) Content Measurements

For the TOC measurements, 2 g of the monomineral sample was weighed and added to 40 mL of deionized water, with the pH adjusted to 9.5, as per the experimental protocol.

The depressant was added according to the flotation reagent scheme, followed by stirring for 5 min to allow a reaction. The mixture was then left to settle for 3 min, after which the supernatant was collected, filtered, and analyzed. The instrument model used was TOC-L CPN.

2.5. Atomic Force Microscopy (AFM) Measurements

A sample of talc ore was selected and sectioned to render both the basal and edge surfaces exposed. The exposed surfaces were sequentially polished using 300-, 600-, 1000-, 3000-, and 5000-grit sandpapers to obtain a smooth surface, followed by 30 min of final polishing to ensure the minimal surface roughness for AFM imaging (Ra < 5 μm). The polished samples were then sealed in a dust-proof box for storage to prevent contamination and ensure sample integrity. The analysis was performed using a Bruker Dimension Icon AFM (Saarbrücken, Germany) in tapping mode, which is ideal for high-resolution surface topography measurements of soft materials like talc.

2.6. Contact Angle Measurements

A bulk talc sample was prepared via cutting to expose the basal and edge planes. The surfaces were sequentially polished using 300-, 600-, 1000-, 3000-, and 5000-grit sandpaper, followed by 30 min of final polishing. The prepared samples were then sealed in a container for preservation. After measuring the initial contact angle of the untreated talc surface, the samples were immersed in a 200 mg/L CMS-Na solution for 5 min, rinsed three times with deionized water, and air-dried for 30 min before further measurements. For talc samples of different particle sizes, the boric acid edge-sealing pellet pressing method was employed for sample preparation. The equipment was a benchtop V1 basic contact angle goniometer, with a measurement accuracy of 0.01°.

3. Results

3.1. Flotation Experiments

Figure 5 illustrates the effect of the pulp's pH on the floatability of talc with different particle sizes. As can be observed in the figure, the flotation recovery of talc generally exceeded 80% within the studied pH range, indicating its strong floatability in the butyl xanthate system. Overall, the −74 + 45 μm particle size fraction exhibited the best floatability, possibly due to the higher proportion of basal surfaces, which enhanced their hydrophobicity. The flotation recovery of the −23 μm fraction was marginally higher than that of the −45 + 23 μm fraction, which can be attributed to the enhanced foam stability of the finer particles and their increased surface energy, leading to more stable attachment to air bubbles [32].

Figure 6 shows the effect of the pulp's pH on talc flotation at different particle sizes in the presence of the depressant CMS-Na. As shown in Figure 6, in a butyl xanthate system with a CMS-Na dosage of 200 mg/L, the floatability of the −74 + 45 μm talc was almost entirely inhibited within the investigated pH range, with a stable recovery rate near 1%, which was unaffected by the pH. The floatability of the −45 + 23 μm talc decreased with increasing pH levels, suggesting that an alkaline pulp environment enhances the inhibition of talc by CMS-Na. At pH = 11.5, the recovery rate dropped to 10.5%. The floatability of the −23 μm talc remained consistently high across the experimental pH range, with a recovery rate of approximately 85% between pH levels of 2 and 10. However, at a pH of 11.5, the recovery rate significantly decreased to 70.3%.

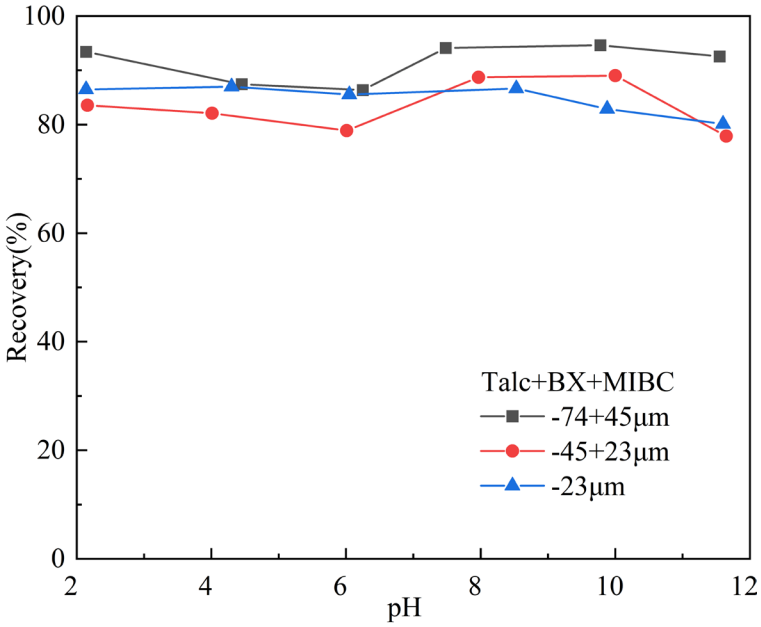


Figure 5. Effect of pulp's pH on the floatability of talc with different particle sizes (BX = 20 mg/L; MIBC = 40 mg/L).

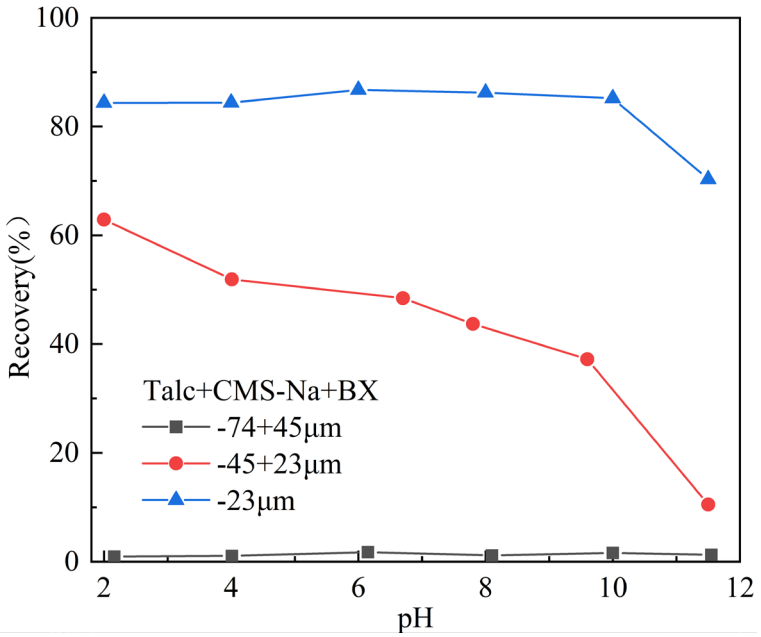


Figure 6. Effect of the pH value on the floatability of talc with different particle sizes under the action of depressant CMS-Na (CMS-Na = 200 mg/L; BX = 20 mg/L; MIBC = 40 mg/L).

Since flotation of copper-nickel ores generally performs better in alkaline environments, a pulp pH of 9.5 was selected for the subsequent experiments. Figure 7 illustrates the effect of the CMS-Na dosage on the flotation performance of talc at different particle sizes. As observed, the flotation recovery of the −74 + 45 μm talc declined significantly with an increasing depressant dosage. As the CMS-Na dosage increased from 0 mg/L to 75 mg/L, the recovery rate dropped from 94.61% to 1.07% and stabilized thereafter. The flotation recovery of the −45 + 23 μm talc began to decrease significantly at a CMS-Na dosage of 100 mg/L, reaching 3.53% at 300 mg/L. The flotation recovery of the −23 μm talc remained over 80% within the selected dosage range. The flotation results suggest that coarser talc

particles are more easily inhibited under the same dosage of depressant, likely due to their more effective interaction with CMS-Na.

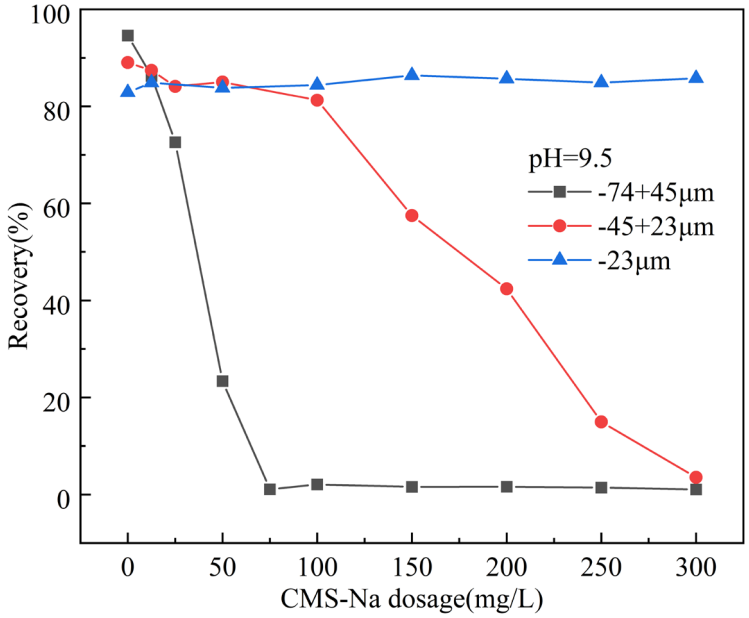


Figure 7. Effect of the depressant CMS-Na dosage on the floatability of talc with different particle sizes (pH = 9.5; BX = 20 mg/L; MIBC = 40 mg/L).

3.2. FTIR Spectral Measurements

The interaction mechanism of CMS-Na on the talc surface was further analyzed through FTIR spectroscopy, and the results are presented in Figure 8, where (a) and (b) show the infrared spectra of butyl xanthate (BX) and carboxymethyl starch sodium (CMS-Na), respectively, with their main absorption peaks and corresponding functional groups.

Figure 8c–e displays the infrared spectra of talc at different particle sizes (−74 + 45 μm, −45 + 23 μm, and −23 μm) before and after treatment with reagents. Taking Figure 8c as an example, the spectrum of the −74 + 45 μm talc showed an absorption peak at 3676.3 cm^{-1}, corresponding to the –OH group. At 1018.4 cm^{-1}, an absorption peak due to the stretching vibration of Si–O–Si was present; and at 671.2 cm^{-1}, a peak caused by the bending vibration of Mg–O appeared [33]. After treatment with BX, the spectrum showed little change, with no characteristic absorption peaks for C=S or C–S, indicating that BX does not significantly adsorb onto talc and suggesting that the natural hydrophobicity of talc surfaces is the primary factor contributing to its flotation. After interaction with CMS-Na, new absorption peaks appeared at 3419.8 cm^{-1} (stretching vibration of –OH), 2929.8 cm^{-1} (stretching vibration of C–H), and 1631.7 cm^{-1} (bending vibration of C=O), indicating that CMS-Na adsorbed onto the talc surface. The C=O absorption peak of CMS-Na shifted from 1647.2 cm^{-1} to 1631.7 cm^{-1}, indicating that the carbonyl group of CMS-Na chemically adsorbed onto the talc surface. In contrast, the –OH absorption peak and C–H absorption peak remained largely unchanged, suggesting that these functional groups were adsorbed onto the talc surface through physical adsorption.

Figure 8f compares the FTIR spectra of the talc samples with varying particle sizes after interaction with CMS-Na and xanthate. As shown in the figure, the –23 μm talc fraction exhibited the strongest CMS-Na absorption peaks, with the most intense C=O characteristic absorption peak being at 1631.7 cm^{-1}, indicating a strong chemical adsorption effect. By magnifying the absorption peaks at 1631.7 cm^{-1} (with equal scaling of the x- and y-axes), it can be observed that the –45 + 23 μm fraction exhibited a moderate adsorption intensity, while the –74 + 45 μm fraction showed the weakest adsorption. This trend was inversely

correlated with the flotation results, where CMS-Na exhibited the poorest depressive effect on the –23 μm talc fraction and the most effective depression on the –74 + 45 μm fraction.

In summary, these findings confirm that talc does not chemically interact with xanthate. CMS-Na adsorbs onto talc through both physical and chemical interactions, with the most pronounced adsorption effect observed on the surfaces of the fine-grained talc.

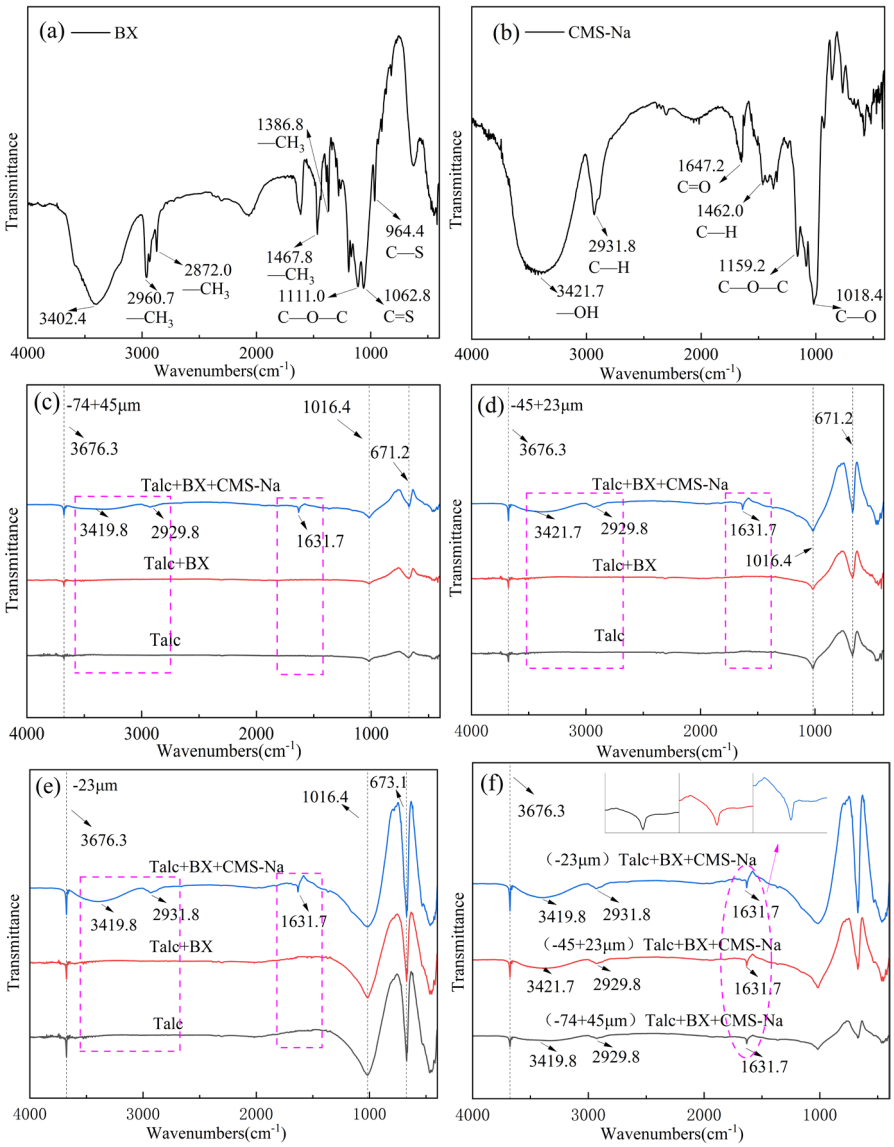


Figure 8. FTIR spectra of talc with varying particle sizes before and after reagents interaction: (**a**) BX; (**b**) CMS-Na; (**c**) −74 + 45 μm talc+BX (CMS-Na); (**d**) −45 + 23 μm talc+BX (CMS-Na); (**e**) −23 μm talc+BX (CMS-Na); and (**f**) −74 + 45/−45 + 23/−23 μm talc+CMS-Na.

3.3. Total Organic Carbon (TOC) Content Measurements

To study the adsorption capacity of CMS-Na on talc of different particle sizes, total organic carbon (TOC) analysis was conducted. Figure 9 presents the TOC content adsorbed on the talc after interaction with CMS-Na at different particle size fractions. As shown in the figure, the adsorption amount of CMS-Na on talc for the −74 + 45 μm fraction was significantly lower than that on the talc for the −45 + 23 μm and −23 μm fractions.

However, in the flotation tests, the talc for the −74 + 45 μm fraction exhibited the strongest depression effect. Based on the FTIR and TOC analysis results, apart from the fact that the fine-grained talc required a higher reagent dosage due to its larger specific surface area and higher surface energy, another underlying mechanism is proposed: As the particle

size decreases, the proportion of talc edge surfaces increases. CMS-Na interacts with metal sites on the edge surfaces through chemical complexation, and the edge surfaces exhibit a stronger affinity for CMS-Na [34,35]. Consequently, fine-grained talc tends to adsorb more of the reagent.

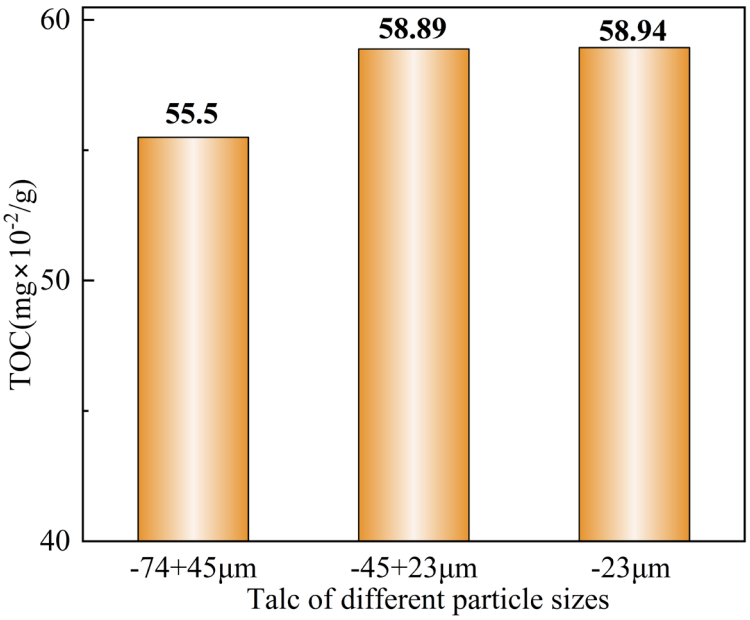


Figure 9. The adsorption capacity of talc at different particle sizes (pH = 9.5).

According to this adsorption mechanism, CMS-Na preferentially adsorbs on the edge surfaces. Given that talc edge surfaces are inherently hydrophilic while the basal surfaces are hydrophobic, even though fine-grained talc adsorbs a larger amount of reagent, the adsorption mainly occurs on the naturally hydrophilic edge surfaces, leaving the basal surfaces hydrophobic. Therefore, fine-grained talc retains good floatability. Under the same reagent dosage, due to the smaller proportion of edge surfaces in coarse-grained talc, a lower amount of reagent was adsorbed on the edges. The remaining reagent was physically adsorbed onto the originally hydrophobic basal surfaces, rendering them hydrophilic and significantly reducing the talc's hydrophobicity. As a result, CMS-Na exhibited the strongest depression effect on talc for the −74 + 45 μm fraction.

3.4. Atomic Force Microscopy (AFM) Measurements

To further verify the aforementioned mechanism analysis, AFM was employed to observe the adsorption behavior of CMS-Na on the basal and edge planes of the talc.

Figure 10(a1,a2) displays the 2D and 3D morphologies of the basal plane of the talc without the reagent, respectively. Due to the low hardness of talc, which makes it prone to surface irregularities during grinding, the surface remained rough even after polishing. However, the overall roughness was relatively low, with an average roughness Ra = 10.9 nm, which was within the acceptable range for the test (Ra < 5 μm).

Figure 10(a3,a4) shows the 2D and 3D morphologies of the basal plane of the talc after treatment with CMS-Na. Following treatment with the reagent, formation of a thin film occurred on the mineral surface, concealing the originally rough and uneven mineral surface. The average roughness of the talc surface decreased to Ra = 4.42 nm, a reduction of 6.48 nm, indicating that a dense CMS-Na polymer layer formed on the talc surface, which resulted in surface smoothing.

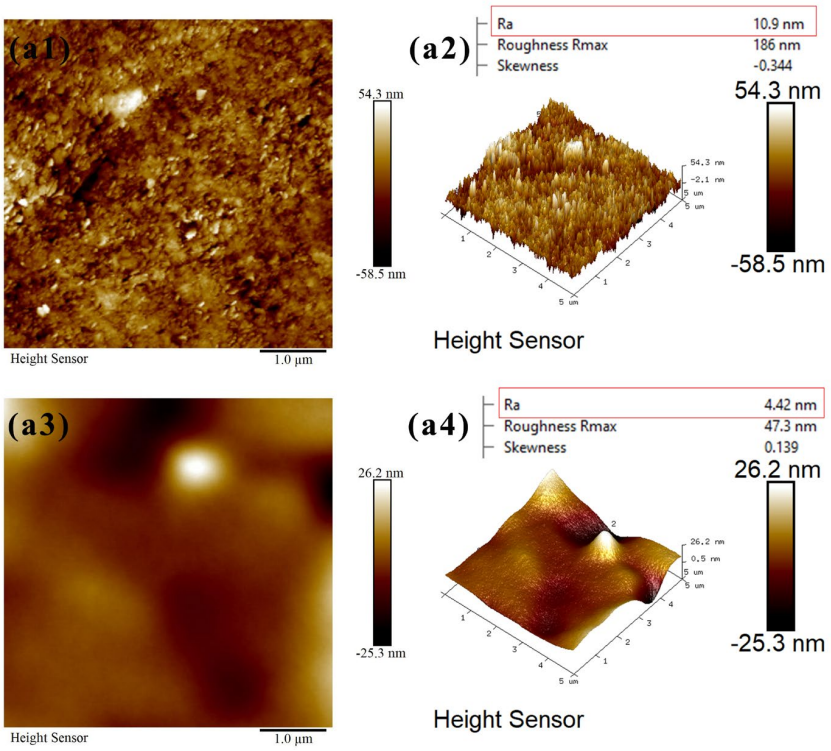


Figure 10. AFM images (left = 2D height images; right = 3D height images) of talc before (**a1**,**a2**) and after (**a3**,**a4**) CMS-Na treatment.

Figure 11(a1,a2) shows the AFM images of the edge surface of the talc, where longitudinal grooves can be observed. The longitudinal grooves are attributed to the anisotropy of the talc crystals, confirming that the surface was indeed the edge plane of the talc. The average surface roughness was 14.3 nm, which met the testing requirements (Ra < 5 µm).

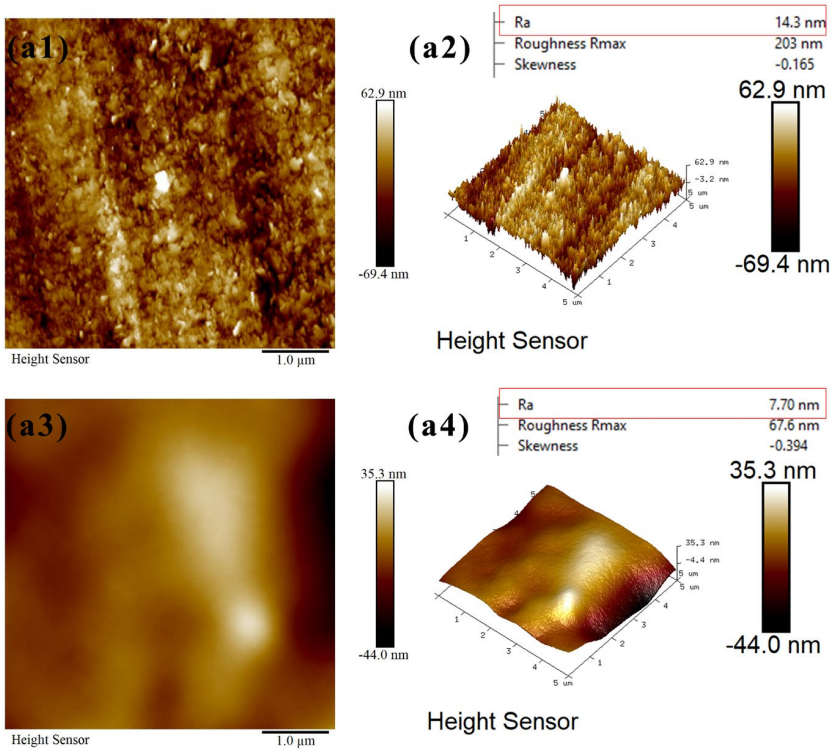


Figure 11. AFM images (left = 2D height images; right = 3D height images) of talc before (**a1**,**a2**) and after (**a3**,**a4**) CMS-Na treatment.

Figure 11(a3,a4) shows the surface morphologies of the talc edge surface after treatment with CMS-Na. Following treatment with the reagent, formation of a thin film occurred on the mineral surface, concealing the originally rough and uneven mineral surface. The average roughness of the talc surface decreased to Ra = 7.70 nm, a reduction of 6.60 nm, suggesting that a dense CMS-Na polymer layer formed on the edge surface.

Compared with the basal planes, the roughness of the edge surfaces underwent more significant changes before and after reagent adsorption, suggesting a stronger adsorption capacity of the edge surfaces for the reagent.

3.5. Contact Angle Measurements

The dissociation of talc during crushing and grinding may lead to changes in the proportion of basal and edge planes, thereby affecting the overall natural floatability of talc due to the distinct properties of its basal and edge surfaces [36,37]. To investigate this, contact angle measurements were conducted for three different particle size fractions, and the results are presented in Figure 12. Since the sample was prepared using a tablet compression method, the measured surface consisted of both the edge and basal planes of the talc. These two surfaces, which exhibited distinct properties, coexisted in a certain proportion and collectively contributed to the measurement surface.

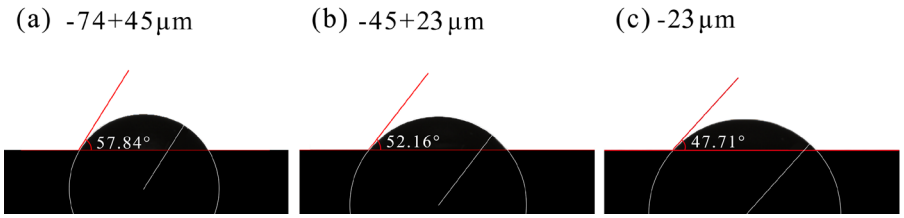


Figure 12. Contact angle photos of different particle sizes of talc: (**a**) −74 + 45 μm, (**b**) −45 + 23 μm, and (**c**) −23 μm.

As was observed, the contact angle of talc for the −74 + 45 μm fraction was 57.84°, that for the −45 + 23 μm fraction was 52.16°, and that for the −23 μm fraction was 47.71°. The contact angle of the talc surface gradually decreased with a decreasing particle size, indicating an increase in hydrophilicity. This suggests that finer-grained talc exposes more edge surfaces, leading to a higher proportion of edge surfaces.

To further investigate the surface wettability differences between the basal and edge surfaces before and after interaction with CMS-Na, contact angle measurements were performed on these surfaces before and after reagent treatment, and the results are presented in Figure 13. As illustrated in the figure, the basal plane's contact angle was 48.46°, while that of the edge surface was 42.26°, indicating that the basal plane was more hydrophobic than the edge plane. After interaction with CMS-Na, the contact angle of the basal plane decreased to 37.68°, representing a reduction of 10.78°, whereas that of the edge plane decreased only slightly to 41.42°, with a reduction of merely 0.84°. CMS-Na interaction with the basal surface significantly enhanced the hydrophilicity of the talc, thereby suppressing its flotation, whereas its interaction with the edge plane resulted in negligible changes in surface wettability.

The contact angle measurements confirm that as the particle size declined, the proportion of edge surfaces increased. Moreover, the influence of CMS-Na on modifying the wettability of the basal plane was much more pronounced than that on the edge surface. Combined with the AFM results, which indicated a stronger adsorption capacity of the edge surface for CMS-Na, these findings validate the previously proposed mechanism: Under the same reagent dosage, CMS-Na preferentially adsorbs onto the edge surfaces of

fine-grained talc. This "ineffective adsorption" is an important factor contributing to the poor depression effect on fine-grained talc.

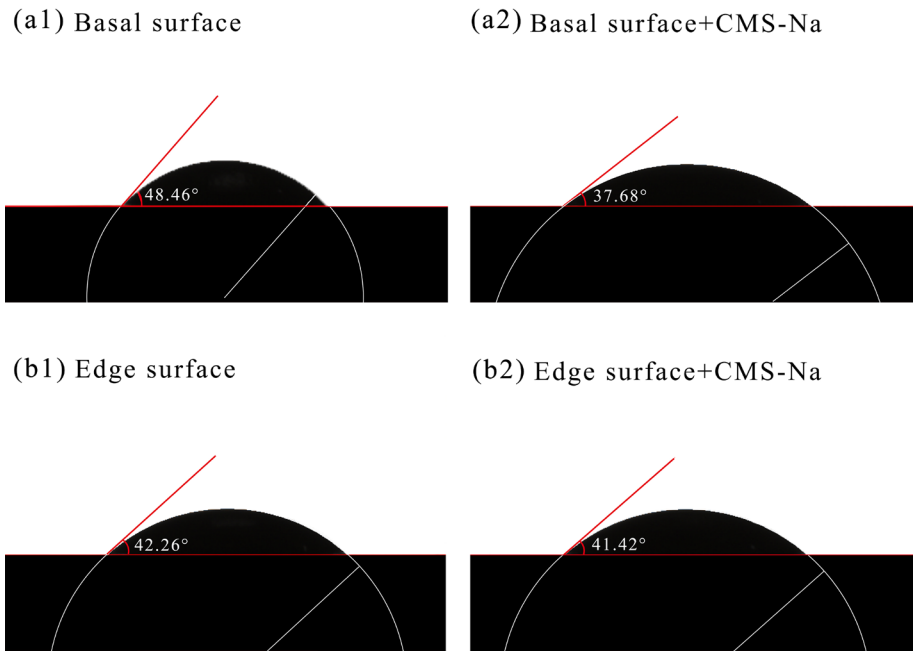


Figure 13. Contact angles of talc on different surfaces before and after interaction with CMS-Na: (**a1**) basal surface, (**a2**) basal surface + CMS-Na, (**b1**) edge surface, and (**b2**) edge surface + CMS-Na.

3.6. Discussion

When talc is crushed and ground, it easily delaminates along the interlayer, forming two completely different dissociation surfaces: the basal plane and the edge plane. The basal plane is a low-energy nonpolar surface with excellent hydrophobicity, while the edge surface is a high-energy nonpolar surface with hydrophilic properties [38]. CMS-Na adsorbs onto a talc surface through both physical and chemical interactions, significantly enhancing the hydrophilicity of the basal surface and thereby suppressing talc flotation.

Mechanism analysis indicates that the interaction between CMS-Na and the basal surface is crucial for increasing talc hydrophilicity. Fine-grained talc exposed more edge surfaces, which exhibited a stronger adsorption capacity for CMS-Na, leading to the adsorption of a large amount of reagent. Under the same reagent dosage, this resulted in a reduced adsorption amount on the basal surface, allowing the talc surface to still retain relatively strong hydrophobicity. This is a key factor contributing to the poor depression effect of fine-grained talc. The interaction mechanism of the reagent with talc of different particle sizes is illustrated in Figure 14.

In actual ores, the talc content can exceed 15%. It is finely disseminated and prone to be enriched in the fine size fraction during the grinding stage, with the majority of the particle sizes being below 38 μm and even reaching below 19 μm [39,40]. Based on the findings of this study, this indicates that in industrial trials, the inhibition of fine-grained talc becomes more challenging.

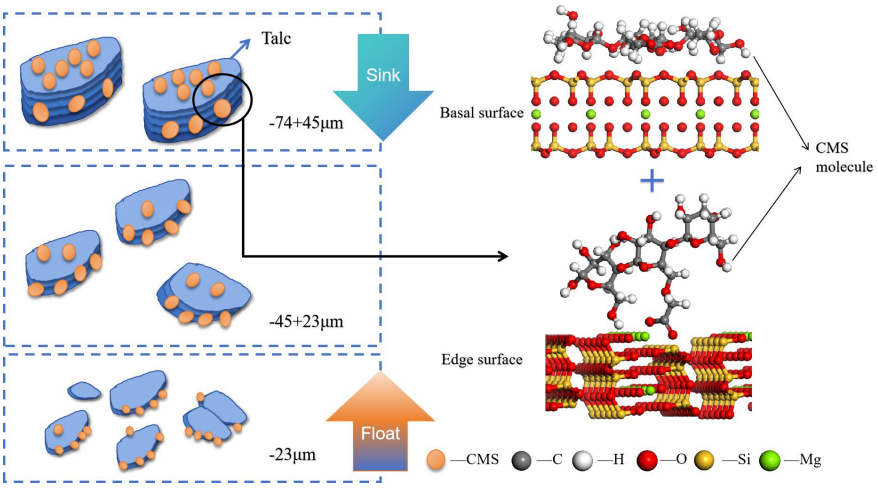


Figure 14. Schematic of the mechanism of CMS-Na on talc of different particle sizes.

4. Conclusions

(1) CMS-Na demonstrated a strong inhibtion influence on talc in an alkaline pulp environment. At a pH of 11.5 and a CMS-Na dosage of 200 mg/L, the recovery of talc in the −74 + 45 μm fraction was 1.27%, while in the −45 + 23 μm fraction, it was 10.5%, and in the −23 μm fraction, it was 70.3%, indicating that CMS-Na is more effective at depressing coarse-grained talc. With an increasing CMS-Na dosage, talc recovery decreased.

(2) FTIR analysis confirmed that CMS-Na was adsorbed on talc through both chemical and physical adsorption, with stronger interactions observed with fine-grained talc. The AFM results indicate that the edge surfaces of talc exhibited a higher adsorption capacity for CMS-Na. Contact angle measurements revealed that with the particle size decreasing, a higher proportion of edge surfaces were exposed, and the effect of CMS-Na on modifying the wettability of the basal surface was significantly greater than its effect on the edge surface.

(3) Under the same CMS-Na dosage and pH conditions, the increased proportion of exposed edge surfaces in fine-grained talc, combined with their stronger adsorption capacity for CMS-Na, led to the adsorption of a large amount of reagent on the edge surfaces. Consequently, the adsorption of CMS-Na on the basal plane was reduced, allowing the talc surface to maintain relatively strong hydrophobicity. This is a key factor contributing to the poor depression effect of fine-grained talc.

Author Contributions: Conceptualization, R.L. and W.D.; methodology, R.L. and W.D.; software, W.M.; validation, W.M., Y.W. and R.L.; formal analysis, W.M.; investigation, W.M.; resources, R.L.; data curation, W.M.; writing—original draft preparation, W.M.; writing—review and editing, Y.W.; visualization, Z.H.; supervision, W.D.; project administration, W.D.; funding acquisition, R.L. All authors have read and agreed to the published version of the manuscript.

Funding: This research was funded by the National Natural Science Foundation of China, grant number No. 52174272.

Data Availability Statement: Data are contained within the article.

Acknowledgments: We are deeply grateful to the three anonymous reviewers for their insightful suggestions, from which we have learned a significant amount.

Conflicts of Interest: The authors declare no conflicts of interest.

References

1. Lu, S. Research on crystal chemistry of talc and review and application of talc flotation in mineral processing of nonferrous sulphide ores. *Min. Metall.* **2010**, *19*, 8–11. [CrossRef]
2. Bai, L. Study on Flotation Kinetics and Separation Mechanism of Talcose Chalcopyrite Ore. Ph.D. Thesis, Mineral Processing Engineering, Northeastern University, Shenyang, China, 2018.
3. Tang, J.; Ma, B.; Li, G.; Zhang, C.; Qi, C. Research situation of development and utilization of talc in china. *Refract. Lime* **2023**, *48*, 10–16. [CrossRef]
4. Farrokhpay, S.; Ndlovu, B.; Bradshaw, D. Behavior of talc and mica in copper ore flotation. *Appl. Clay Sci.* **2018**, *160*, 270–275. [CrossRef]
5. Jin, S.; Zhang, P.; Ou, L. Study on the depression mechanism of zinc sulfate on talc in chalcopyrite flotation. *Colloids Surf. A Physicochem. Eng. Asp.* **2021**, *619*, 126474. [CrossRef]
6. Yi, H.; Zhao, Y.; Rao, F.; Song, S. Hydrophobic agglomeration of talc fines in aqueous suspensions. *Colloids Surf. A Physicochem. Eng. Asp.* **2018**, *538*, 327–332. [CrossRef]
7. Huangfu, Z.; Sun, W.; Zhang, H.; Chen, C.; Zhang, C. Hydrophilic modification of macroscopically hydrophobic mineral talc and its specific application in flotation. *Langmuir* **2024**, *40*, 25988–25996. [CrossRef] [PubMed]
8. Ou, L.; Qi, C. Depressing of polysaccharides in floating separation of talc from molybdenite of non-polar surface minerals. *Met. Mine* **2015**, *5*, 85–89. [CrossRef]
9. Feng, Q.; Zhang, C.; Zhang, G.; Liu, C.; Shi, Q. Effect of carboxylation chitosan on flotation behaviors of talc in presence of calcium ions. *Chin. J. Nonferrous Met.* **2018**, *28*, 1191–1195. [CrossRef]
10. Zhong, C.; Feng, B.; Yan, H.; Liu, Y.; Liu, G.; Cheng, Y.; Ning, X.; Wang, H. Effects of three organic depressants on flotation separation of molybdenite and talc. *Chin. J. Nonferrous Met.* **2022**, *32*, 3843–3852. [CrossRef]
11. Li, J.; Kong, L.; Lv, J.; Wei, M. Reaction mechanism and research progress of organic depressants on talc in flotation of sulfide ores. *Conserv. Util. Miner. Resour.* **2023**, *43*, 171–178. [CrossRef]
12. Feng, B.; Zhang, W.; Guo, Y.; Peng, J.; Ning, X.; Wang, H. Synergistic effect of acidified water glass and locust bean gum in the flotation of a refractory copper sulfide ore. *J. Clean. Prod.* **2018**, *202*, 1077–1084. [CrossRef]
13. Li, J.; Ma, Y.; Li, G.; Liu, Z.; Ning, S.; Pei, B.; Lang, B.; Liu, R.; Liu, D. Depression mechanism of $ZnSO_4$ and Na_2CO_3 on talc flotation. *Trans. Nonferrous Met. Soc. China* **2023**, *33*, 1559–1571. [CrossRef]
14. Feng, B.; Peng, J.; Zhang, W.; Ning, X.; Guo, Y.; Zhang, W. Use of locust bean gum in flotation separation of chalcopyrite and talc. *Miner. Eng.* **2018**, *122*, 79–83. [CrossRef]
15. Wu, W.; Chen, T.; Shao, Y.; Ye, G.; Xiong, T. The flotation separation of molybdenite from talc using zinc sulfate in sodium silicate system and related mechanism. *Colloids Surf. A Physicochem. Eng. Asp.* **2022**, *641*, 128451. [CrossRef]
16. Pan, G.; Shi, Q.; Zhang, G.; Huang, G. Selective depression of talc in chalcopyrite flotation by xanthan gum: Flotation response and adsorption mechanism. *Colloids Surf. A Physicochem. Eng. Asp.* **2020**, *600*, 124902. [CrossRef]
17. Zeng, G.; Chen, W.; Yang, L.; Liu, S.; Liu, G. Understanding the role of calcium lignosulphonate in flotation separation of chalcopyrite from talc. *Miner. Process. Extr. Metall. Rev.* **2024**, *45*, 881–891. [CrossRef]
18. Ma, X.; Pawlik, M. The effect of lignosulfonates on the floatability of talc. *Int. J. Miner. Process.* **2007**, *83*, 19–27. [CrossRef]
19. Shortridge, P.G.; Harris, P.J.; Bradshaw, D.J.; Koopal, L.K. The effect of chemical composition and molecular weight of polysaccharide depressants on the flotation of talc. *Int. J. Miner. Process.* **2000**, *59*, 215–224. [CrossRef]
20. Yu, Z.; Sun, Z.; Wang, L.; Ye, Y. Research on new beneficiation technology for refractory molybdenum ore with high talc content. *Nonferrous Met. Miner. Process. Sect.* **2024**, *7*, 102–109. [CrossRef]
21. Li, C.; Wang, C.; Wu, F.; Zhu, G.; Cao, Y.; Cao, S. Flotation separation of molybdenite from talc using carrageenan as depressant. *Miner. Eng.* **2025**, *222*, 109122. [CrossRef]
22. Zhong, C.; Wang, H.; Zhang, L.; Guo, M.; Feng, B. Flotation separation of molybdenite and talc by xanthan gum. *Powder Technol.* **2021**, *388*, 158–165. [CrossRef]
23. Zhou, H.; Zhang, Z.; Ou, L.; Mai, Q. Flotation separation of chalcopyrite from talc using a new depressant carrageenan. *Colloids Surf. A Physicochem. Eng. Asp.* **2020**, *603*, 125274. [CrossRef]
24. Zhao, K.; Gu, G.; Wang, C.; Rao, X.; Wang, X.; Xiong, X. The effect of a new polysaccharide on the depression of talc and the flotation of a nickel–copper sulfide ore. *Miner. Eng.* **2015**, *77*, 99–106. [CrossRef]
25. Sheng, Q.; Yin, W.; Ma, Y.; Liu, Y.; Wang, L.; Yang, B.; Sun, H.; Jin, Y. Selective depression of talc in azurite sulfidization flotation by tamarind polysaccharide gum: Flotation response and adsorption mechanism. *Miner. Eng.* **2022**, *178*, 107393. [CrossRef]
26. Liu, X.; Zhang, X.; Zhang, Y.; Xu, X.; Ning, S.; Zuo, Q.; Fang, J.; Shen, P.; Liu, D. Welan gum as a new depressant for the flotation separation of chalcopyrite from talc. *Chem. Phys.* **2024**, *578*, 112139. [CrossRef]
27. Liu, C.; Qi, Z.; Ren, L.; Yang, S. The selective adsorption mechanism of calcium ions/pullulan in the flotation separation of chalcopyrite from talc. *Chem. Eng. Sci.* **2025**, *302*, 120819. [CrossRef]

28. Ye, W.; Zhang, X.; Pan, C.; Hu, X.; Luo, Y.; Xu, P. Selective flotation separation of chalcopyrite from talc by a novel depressant: N-methylene phosphonic chitosan. *Miner. Eng.* **2022**, *177*, 107367. [CrossRef]
29. Huangfu, Z.; Sun, W.; Zhu, H.; Liu, R.; Cheng, C. Selective depression of biodegradable talc depressant sodium carboxymethyl starch on molybdenite flotation with sodium diethyldithiocarbamate. *Sep. Purif. Technol.* **2025**, *352*, 127950. [CrossRef]
30. Liu, C.; Zhang, W.; Song, S.; Li, H. A novel method to improve carboxymethyl cellulose performance in the flotation of talc. *Miner. Eng.* **2019**, *131*, 23–27. [CrossRef]
31. Pan, G.; Lu, Y.; Feng, Q.; Long, T. Effect of sodium carboxymethyl cellulose on flotability and dispersion of talc. *Met. Mine* **2010**, *39*, 96–100.
32. Xue, W.; Liang, Y. Study on the foam stability and flotation behavior of talc. *Non-Met. Miner.* **1994**, *04*, 21–23.
33. Gui, W.; Lei, D.; Wang, Y.; Zhang, S.; Zhao, X.; Tian, J. Inhibition mechanism of lead ions synergized with malic acid on talc. *Conserv. Util. Miner. Resour.* **2023**, *43*, 86–94. [CrossRef]
34. Liu, G.; Feng, Q.; Ou, L.; Lu, Y.; Zhang, G. Adsorption of polysaccharide onto talc. *Miner. Eng.* **2006**, *19*, 147–153. [CrossRef]
35. Zhan, W.; Yang, S.; Bao, S.; Ren, L.; Liu, C. A novel insight of interaction mechanism of carboxymethyl cellulose with talc surface: A combined molecular dynamic simulation and DFT investigation. *Appl. Clay Sci.* **2024**, *247*, 107201. [CrossRef]
36. Xue, J.; Tu, H.; Shi, J.; An, Y.; Wan, H.; Bu, X. Enhanced inhibition of talc flotation using acidified sodium silicate and sodium carboxymethyl cellulose as the combined inhibitor. *Int. J. Miner. Metall. Mater.* **2023**, *30*, 1310–1319. [CrossRef]
37. Xie, Y.; Yin, W.; Yao, J.; Yin, X.; Liu, J.; Xue, F.; Tian, D. Flotation behavior and surface adsorption mechanism of a novel selective inhibitor HDP in the separation of chalcopyrite and talc flotation. *J. Mol. Liq.* **2024**, *398*, 124206. [CrossRef]
38. Ann Bazar, J.; Rahimi, M.; Fathinia, S.; Jafari, M.; Chipakwe, V.; Chehreh Chelgani, S. Talc flotation—An overview. *Minerals* **2021**, *11*, 662. [CrossRef]
39. Li, G.; Ren, X.; Zhang, W.; Yu, J. Process mineralogical study of comprehensive tailings from nanfen concentrator. *Mod. Min.* **2024**, *40*, 119–123.
40. Cao, Y.; Sun, L.; Sun, W.; Wang, Q.; Wang, C.; Peng, Z.; Gao, Z.; Cao, X. Flotation test study on low-grade sulfide copper-nickel ore with high slime and high magnesium content. *Min. Metall. Eng.* **2023**, *43*, 62–65. [CrossRef]

Disclaimer/Publisher's Note: The statements, opinions and data contained in all publications are solely those of the individual author(s) and contributor(s) and not of MDPI and/or the editor(s). MDPI and/or the editor(s) disclaim responsibility for any injury to people or property resulting from any ideas, methods, instructions or products referred to in the content.